

Application of EMD-Based TVAR Model for Modal Analysis of Semi-submersibles

Edwar Yazid, M. Shahir Liew, Setyamartana Parman, V.J. Kurian and C.Y. Ng

Abstract—This paper presents a technique for using a parametric approach for modal properties estimation of a floating offshore structure. The technique utilizes empirical mode decomposition (EMD)-based time-varying autoregressive (TVAR) model, which is an extended form of the well-known AR model. Input for TVAR model is surge motion as system response, obtained experimentally from a scaled 1:40 model of a prototype semi-submersible. By utilizing the advantage of time-varying spectrum generated from TVAR model, estimation of the modal properties is carried out in the time-frequency plane via poles technique under different random wave spectrum. The results show that the modal frequency and its corresponding damping ratio for surge motion either in low frequency or wave frequency region can be estimated well. The Stochastic subspace identification method and free-decay test of the semi-submersible prototype are taken as benchmark.

Keywords— EMD, Modal Analysis, Semi-submersible, TVAR model.

I. INTRODUCTION

THE work presented in this paper is motivated by the fact that accurate modal analysis is very important for predicting the dynamic characteristics of a structural system. In the sense of offshore structures, the modal analysis has essential impact on offshore monitoring campaign, damage assessment and fatigue analysis. It is also the base for updating or calibration of mathematical model of a structural system. Related recent researches in this field are the introduction of Prony's method to the offshore community by [1]-[2], where they employed it for jacket-type platform using the measured free-vibration data.

However, researches concerning the modal parameters identification on offshore floating structures are rare. The offshore community is not aware of any work on the extraction of modal properties based on the available measured data either measured motion responses only or transfer function generated from wave height and motion responses of the respective floating structures. Hence, the purpose of this paper is to address this problem. In this paper, attention is focused on the estimation of modal properties of a semisubmersible model, representing a floating offshore structure by

introducing the parametric approach. The primary interest lies in the surge motion due to second-order nonlinear effect is pronounced in that motion.

The idea is to try to simplify the modal properties estimation by decomposing the surge response into its wave frequency (WF) and low frequency (LF) response corresponding to surge motion of semisubmersible model as well as noise elimination embedded in the measured surge response. The decomposition process enables the modal analysis become easier. Modal estimation can then be solved by introducing the application of the TVAR model for output-measurement only via time-varying spectrum. To support the results, surge motion free-decay test and stochastic subspace identification method are taken as benchmark.

II. MATHEMATICAL FORMULATION

A. Empirical Mode Decomposition (EMD)

The essence of empirical mode decomposition is to decompose signal $y(t)$ into its oscillatory mode, called intrinsic mode function (IMF). This is achieved by sifting process. A step by step procedure of EMD can be summarized as follows:

- I. Identify all the local extrema, maxima and minima of $y(t)$, and then connect the local maxima and minima using the cubic spline to obtain the upper and lower envelope, respectively. Those envelopes should cover all the data of $y(t)$. Their mean is designated as m_I , and the difference between $y(t)$ and m_I is defined by

$$h_I = y(t) - m_I. \quad (1)$$

Ideally, h_I should be an IMF if it satisfies two conditions: i) in all data of $y(t)$, the number of extrema and zero crossings must be either be equal or differ at most by one; and ii) at any point, the mean value of the envelope defined by the local maxima and minima is zero.

- II. If h_I does not satisfy the conditions, set h_I as the original data and repeat the process in I until the conditions are fulfilled and the first IMF is achieved.
- III. Residue is then subtracted from II, taken as original signal and sifting process is repeated to obtain another IMF. The process is repeated until n IMF is obtained,

Edwar Yazid. Author is with the Mechanical Engineering Department, Universiti Teknologi Petronas, Bandar Seri Iskandar, Tronoh, Perak, Malaysia, 31750 (corresponding author to provide phone: 6053657197; fax: 6053656461; e-mail: edwar.putra@gmail.com).

where relationship between IMFs and the original data $y(t)$ may be expressed as

$$y(t) = \sum_{i=1}^n c_i(t) + r_n(t). \quad (2)$$

Term $c_i(t)$ contains the IMFs of the $y(t)$, from high to low frequency components. Each $c_i(t)$ also contains a different frequency component, while $r_n(t)$ is the residual which is the trend of the data or a constant.

In practice, sifting process produces an IMF which contains more than natural frequency components. This is called mode mixing, because of some drawbacks in EMD algorithm. The mode mixing must be avoided for the goal of this paper. Reference [3] has proposed intermittent frequency to avoid the mode mixing. In their work, the intermittency is based on the period length to separate the time series into different modes. The criterion frequency is set as the upper limit of the period that can be included in any given IMF component, so that the resulting IMF will not contain any natural frequency components smaller than the intermittent frequency. However, the intermittent frequency as an additional criterion might not always guarantee the final expected results, since choosing the intermittent frequency is a subjective task. Further, author in [4] has solved this problem by proposing some modifications on the EMD algorithm. Their finding results show that some issues related to the drawbacks of EMD algorithm can be solved, such as mode mixing. This reference is the recent work in EMD algorithm; hence it will be adopted for decomposing the surge motion.

B. TVAR Model

TVAR model estimates time-varying spectrum by modeling the signals as a time-series. Such a model is an extended form of the well-known AR model, where in the TVAR the coefficients are time-variant. AR model is not discussed here, due to the theory is mature and available in many system identification literatures. Shortly, TVAR is given by:

$$y(k) = \sum_{i=1}^N a_i(k)y(k-i) + e(k). \quad (3)$$

Term $y(k-i)$ is delayed time series, called regressors. Notation N is number of delayed regressors which are the order of TVAR model. Values $a_i(t)$ are the TVAR coefficients which is time-variant. Model error is noted by $e(k)$, which is Gaussian with zero mean and variance σ_e^2 . From (3), the work is mostly concerned with the identification of coefficients $a_i(t)$. Equation (1) reflects that the current measured output depends on previous states of output and model error. Rewriting (3) in a discrete state-space form, which is convenient for formulating adaptive filters, the coefficients may be estimated as expressed in (4a),

$$y(k) = x(k)L(k) + v(k) \quad (4a)$$

$$L(k) = AL(k-1) + w(k). \quad (4b)$$

Vector $x(k)$ contains the regressors, past values measurement $[y(k-1), \dots, y(k-N)]$, while vector $L(k)$ contains the TVAR coefficient values. If time evolution of the coefficients is restricted to be linear and stochastic, then $L(k)$ is then expressed in (4b). Term A is the state transition matrix which will be restricted as identity matrix, while $v(k)$ and $w(k)$ are the observation and state noise, respectively. Error minimization between the models' simulated output in (3) and the measured data can be accomplished by adopting several methods. Because the floating offshore structures are dynamic system with slow variations, adaptive methods can be utilized. For more detail about those methods, one may refer to [5].

C. Time-Varying Spectrum

After obtaining the coefficients, it can be converted into time-varying spectrum and expressed in (5).

$$H(k, s) = \frac{\sigma_e^2}{\left| 1 - \sum_{i=1}^p a_i(k)e^{-si} \right|^2}. \quad (5)$$

Terms in (5) are explained as follows: $s = j\omega$ where ω is the observed frequency, $a_i(k)$ is the i^{th} element of the estimated coefficients and f is the observed frequency, respectively. Poles of the system can be obtained by factoring the denominator of (5) and expressed in (6).

$$H(k, s) = \frac{\sigma_e}{(s - p_1(k))(s - p_2(k)) \dots (s - p_N(k))}. \quad (6)$$

The number of poles is determined by the number past observations of the measured output included in the model. The "poles" of the system can be drawn in the complex plane. The location of both on the complex plane yields useful information regarding the properties of the system, namely modal property. Denominator of (6) is known as characteristic equation which defines properties of the entire system. As in [6], the amplitude of a pole is related to the damping ratio ζ and the phase of the poles is related to the frequency f , expressed in (7) below,

$$f_i(k) = |\ln p_i(k)| \cdot \frac{Fs}{2\pi} \quad (7a)$$

$$\zeta_i(k) = -\cos(\arg(\ln p_i(k))) \quad (7b)$$

Notation λ_i is the i -th discrete-time poles and F_s is sampling frequency.

III. EXPERIMENTAL SET-UP

The method is then applied to the case of a twin hulled semi-submersible model with eight circular columns as displayed in Fig. 1. The model was designed with scale of 1:40 to fit the wave tank and was fabricated by using acrylic plate. In this study, an assumption was made that the model follows the Froude’s law of similitude. The principal dimensions for the prototype and the model are listed in Table 1. The model test was moored with two typical springs that attached with steel wires on fore and aft side of the model.

Table 1: Typical dimension of semisubmersible (scale 1:40)

| Element | Designation | Prototype (m) | Model (m) |
|---------|------------------------|---------------|------------|
| Pontoon | Length | 44 | 1.1 |
| | Breath | 6 | 0.15 |
| | Depth | 3.2 | 0.08 |
| Column | Diameter | 3.2 & 4 | 0.08 & 0.1 |
| | Spacing (longitudinal) | 9.6 | 0.24 |
| | Spacing (transverse) | 2.4 | 0.6 |
| | Draft | 8 | 0.2 |

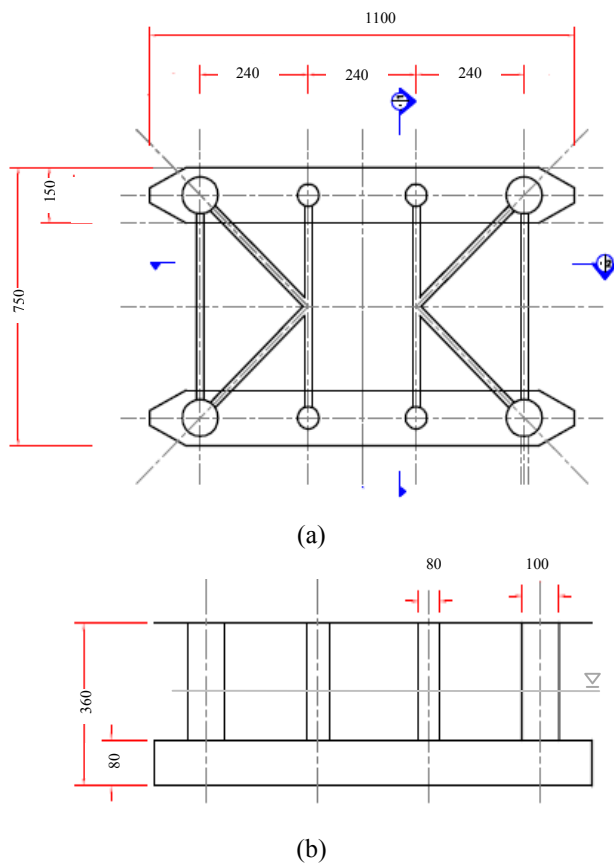


Fig. 1 Principal dimensions of the model (in mm) (a) plan of the scaled model (b) section of the scaled model

The springs were soft linear springs connected to load cells mounted on the model. This arrangement was set up to measure the second-order motion response. This was made possible by the soft spring wire restraining system attached to

the model [7]. This arrangement allowed the model to respond to the wave loading in six degrees of freedom.

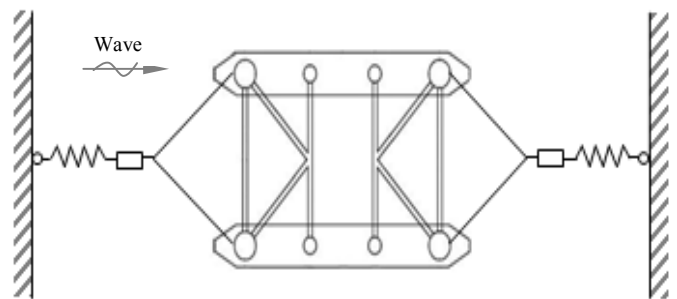


Fig. 2 Plan of the set-up

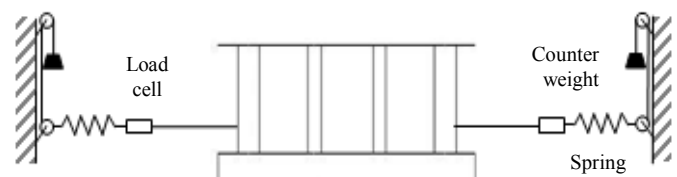


Fig. 3 Section of the test set-up

The model was then tested in the wave tank of the offshore engineering laboratory, Universiti Teknologi PETRONAS. The wave tank has 22 m length, 10 m width and 1.5 m depth. The JONSWAP spectrum was used to generate the random wave, where the test was conducted for six minutes duration and the model was subjected a unidirectional random wave in head seas orientation. Wave probes were used to measure the wave height, while the motion responses of the semi-submersible model in all the six-degree-of-freedom were recorded by optical tracking system. The test took only few minutes, hence the effects of wave wall reflection were not considered. The progressive mesh beach systems also minimized the interference from reflected waves during tests. The data had been sampled at sampling frequency 100 Hz. Pre-processing for all data set is carried out for both original measured time series and described in the next section.

In addition, four sets of random wave used are shown in Table 2. The wave frequency and the wave heights are taken based upon the limitation of the wave tank and wave maker. Peakedness parameter of the JONSWAP wave spectrum is 2.

Table 2: Random wave parameters

| Data | Significant Height (m) | Peak Frequency (Hz) |
|-------|------------------------|---------------------|
| IRW-1 | 0.06 | 0.83 |
| IRW-2 | 0.08 | 0.77 |
| IRW-3 | 0.09 | 0.71 |
| IRW-4 | 0.1 | 0.61 |

IV. RESULTS

In this section, application of the proposed method in modal properties estimation is demonstrated. Two processes are carried out to accomplish the goal in this paper, namely raw data processing and decomposition process. Both will be discussed in the next section, by taking IRW-4 and its surge response time series as a sample.

A. Raw Data Processing

The raw measured time histories of wave height and surge response are presented in Fig. 4. In order to make sure that either WFR or LFR exist in the measured data, FFT is then applied. This information is important to identify the frequency range for decomposition process. The obtained results are presented in Fig. 5.

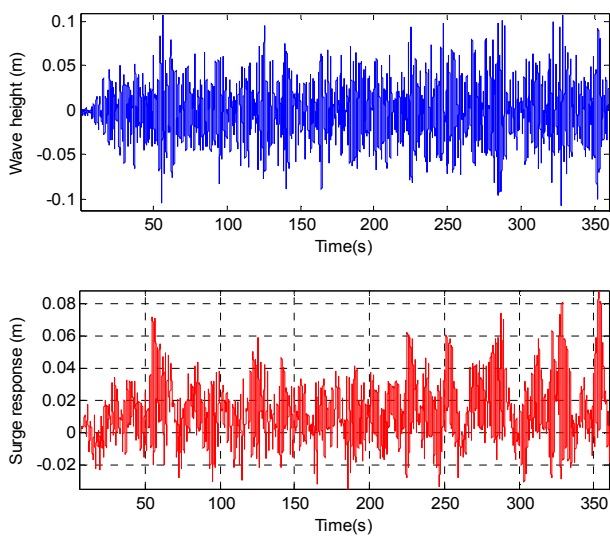


Fig. 4 Wave height and surge response of IRW-4

From the figure, we can observe that the wave height appear to be symmetrical, while the surge response is not symmetrical and seems to be shifted upward. In order to make sure that either WFR or LFR exist in the measured data, FFT is then applied. This information is important to identify the frequency range for decomposition process. Most of wave energy is in the range $0.3 < f < 1.5$ Hz, as depicted in the right column of Fig. 5(a). In the right column of Fig. 5(b), the FFT of surge response has two principal frequency peaks. The first peak is in the low frequency region at around 0.05 Hz, approximately 0.07 Hz, which is close to the surge natural frequency of the semi-submersible model.

This frequency may be called as the resonant low frequency (LF). The second peak is around 0.61 Hz, corresponds to the frequency exist in the random wave spectrum. This frequency is known as incident wave frequency (WF). Contrary with Fig. 5(a), the resonant LF is not present in the wave spectrum. Direct assessment may be drawn directly from the results above, that the semi-submersible model is nonlinear system. These finding results are also found by many prior researches, for example [8]-[10]. In addition, Fig. 5 also provides

information that both measured time series are contaminated with noise.

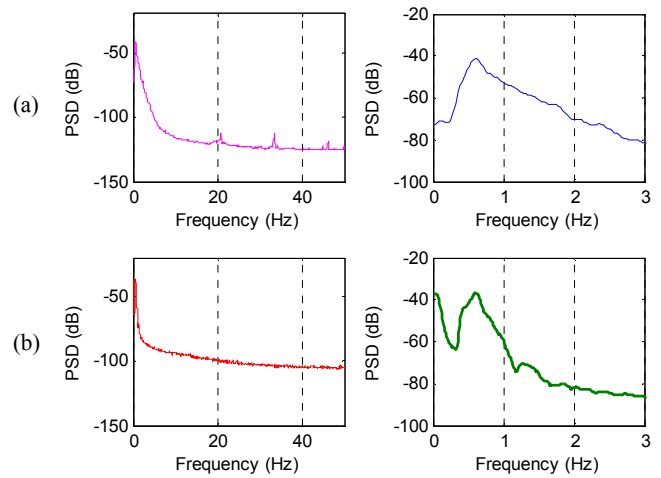
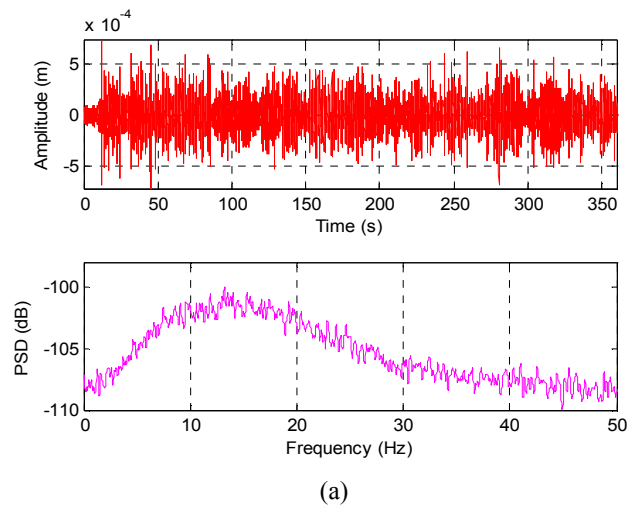


Fig. 5 FFT for (a) IRW-4 data (b) its surge response

B. Decomposition Process

Further, based on the results of Fig. 5, decomposition of measured time series of surge response is carried out. This is to identify LF and WF motion in time domain by adopting using empirical mode decomposition (EMD) method developed by [4]. Results are depicted in Fig. 6. As shown in Fig. 6, decomposition result can be classified into three IMFs. Each IMF in Fig. 6 can be interpreted as follows:

- i) The first IMF is identified as measurement noise during the experiment. If low pass filter (LPF) with cut-off frequency, 0.01 Hz is applied as filter for raw measured surge response, the noise embedded in the time series will be the same with first IMF. This finding result also confirms that EMD method may be used as an alternative filter tool for noisy time series.
- ii) The second IMF is identified as a wave frequency motion and confirmed with its FFT result.
- iii) The third IMF is identified as low frequency motion as confirmed by FFT result.



(a)

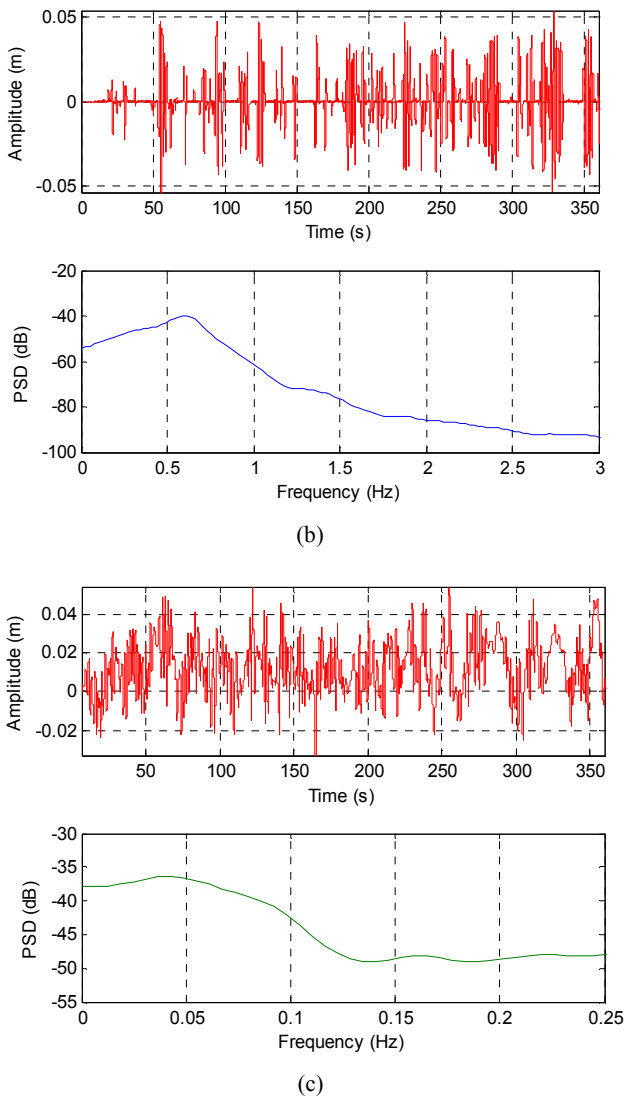


Fig. 6 Time series and spectrums of decomposed surge motion (a) IMF and spectrum of the noise (b) IMF and spectrum of the LFR (c) IMF and spectrum of the WFR

Results from Fig. 6 are basis for the modal parameters estimation. This simply illustrate that estimation is carried out either in LF or WF region although surge motion is one mode. In this stage, several modal analysis methods may be employed such as pick picking method, Prony’s method, stochastic subspace identification (SSI) method including the proposed method.

In order to increase the computational efficiency and performance of the proposed method, data length reduction is carried out by down sampling. Down sampling is accomplished by resampling both time series in the important frequency range, $0 < f < f_{max} = 1.5$ Hz as shown in the Fig. 5. New sampling frequency can be obtained by $F_s = 2 \cdot f_{max} = 3$ Hz. This new sampling frequency reduces the original data from 39445 data points into 1080 data points without loss of the important frequency content.

C. Modal Analysis

Before conducting the modal analysis, free decay analysis is carried out. Free-decay physical measurement for surge motion is shown in Fig. 7. The decay test was conducted in still water by giving an initial displacement and the subsequent motions were recorded. The natural frequency and damping ratio of the model in surge are estimated from the free-decay test using the logarithmic decrement formula and the results are listed in Table 3.

Table 3: Natural frequency and damping ratio of the model

| Motion | Natural frequency (Hz) | Damping ratio (%) |
|--------|------------------------|-------------------|
| Surge | 0.07 | 11.3 |

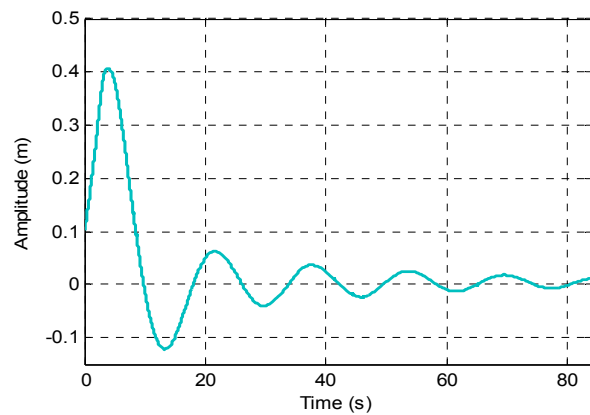
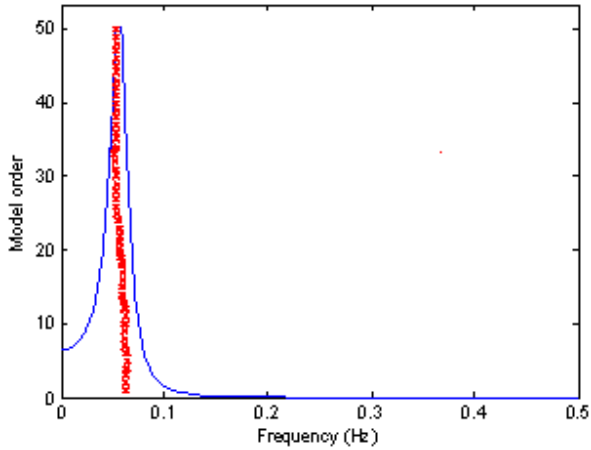


Fig. 7 Surge free-decay result

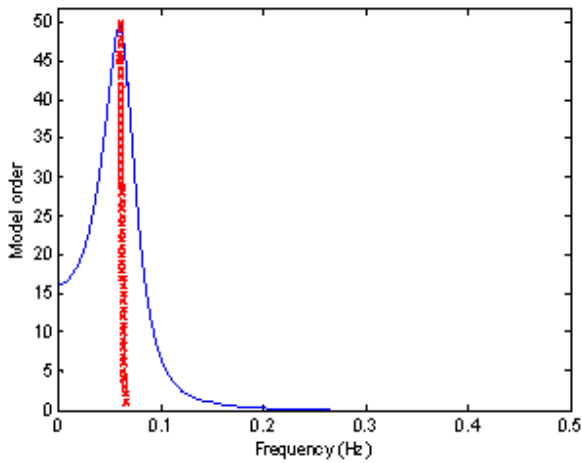
After measurement of surge motion surge response of IRW-4 has been decomposed, the data are ready for the modal parameters identification. The calculated TVAR stabilization diagrams of the two decomposed two IMFs (IMF of LFR and WFR) are presented in Fig. 8- 9. The stabilization diagrams use model order from 2 up to 50 and consist of 1 curve and one symbol. Symbol with x-mark (‘x’) is identified stable pole. Every curve in those figures with solid line (‘-’) is averaged transfer function. The transfer function is calculated using (5). To create this curve, model order of 2 is used. We can observe that TVAR model produces smooth spectrums, means that the method provides good frequency resolution.

It can be clearly seen from Fig. 8-9, that each TVAR stabilization diagram of the decomposed two IMFs demonstrates one clear stable pole. The stable poles in the decomposed TVAR model stabilization diagram make the modal parameter identification much easier. It is worth to note that the diagram is constructed based on (7a). For clearance, the identified modal frequencies of the semi-submersible by using the proposed EMD-based TVAR model technique are summarized in Table 4 and compared with those obtained from SSI method. In WF region, modal frequencies are consistent with their corresponding wave spectrums as seen in Table 2. In LF region, the modal frequencies are also consistent around 0.05 Hz for every wave spectrums, which

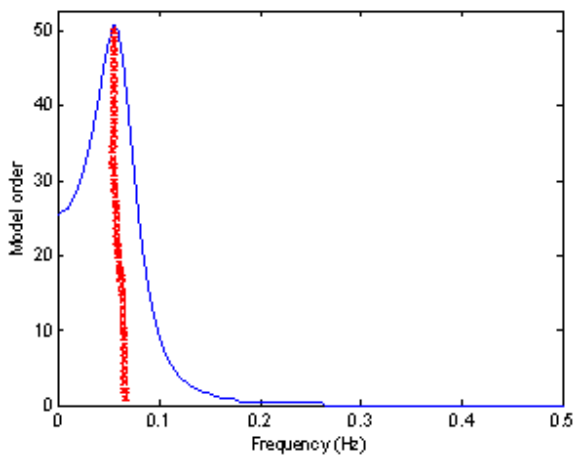
confirms that the variation of wave spectrum frequency does not affect the low frequency of floating structures. Modal damping ratios in WF and LF region can be calculated using (7b). The values are tabulated in Table 5. In WF region, it can be found out that damping ratios are not sensitive to the variation of wave spectrum frequency. This is to be expected since in WF region, first-order wave motion is dominant.



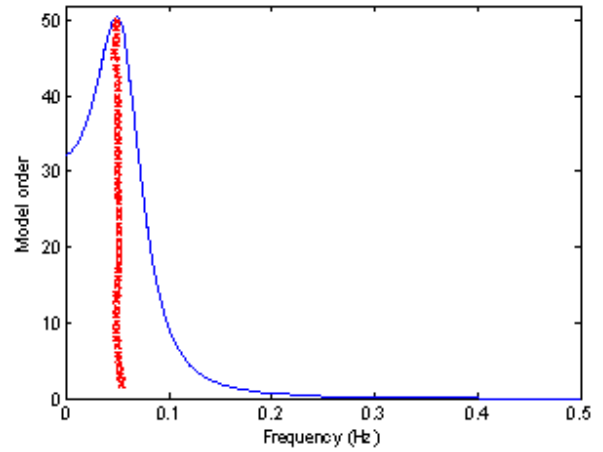
(a)



(b)



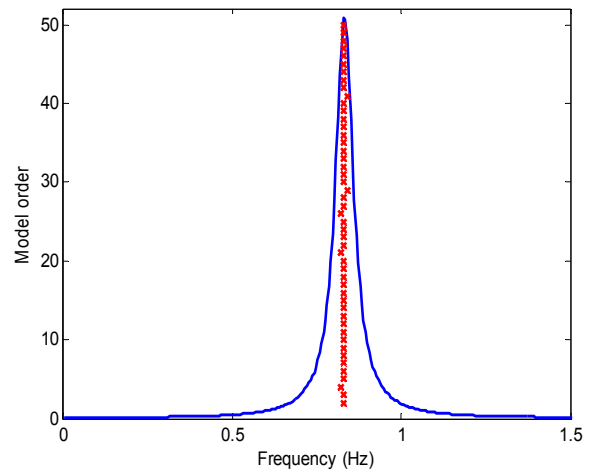
(c)



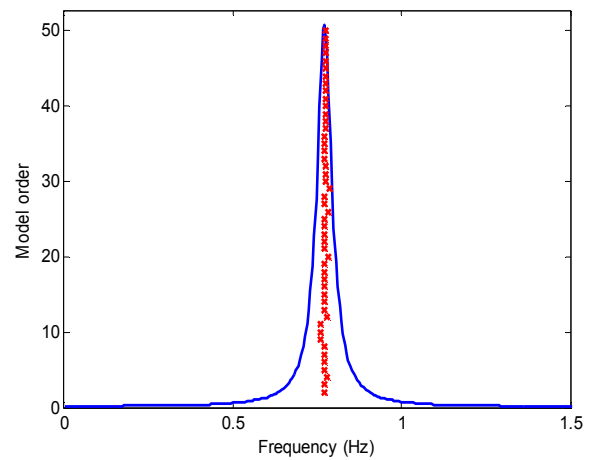
(d)

Fig. 8 TVAR stabilization diagram for LFR (a) IRW-1 (b) IRW-2 (c) IRW-3 (d) IRW-4

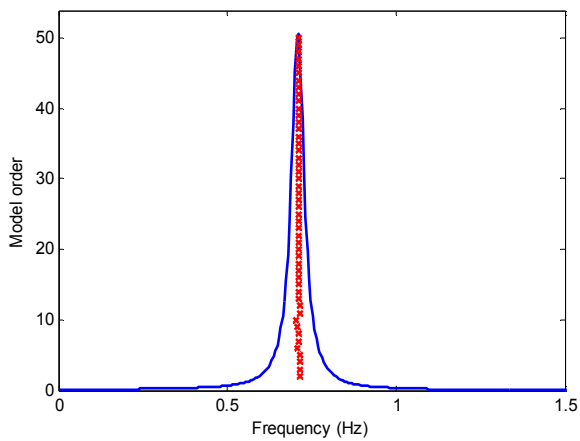
Those values are lower with value obtained from free-decay test, where the ratio is almost twice.



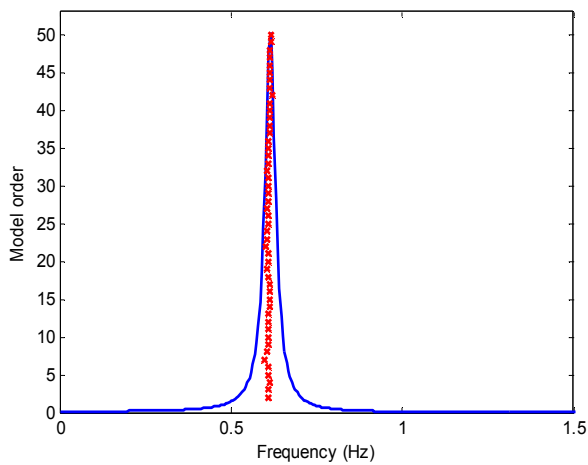
(a)



(b)



(c)



(d)

Fig. 9 TVAR stabilization diagram for WFR (a) IRW-1 (b) IRW-2 (c) IRW-3 (d) IRW-4

As shown in LF region, damping ratio slightly changes to higher value as the wave frequencies increase. The values are about 5.81%, 12.44 %, 14.34 % and 20.55% higher than that in the free-decay test in Table 3, respectively.

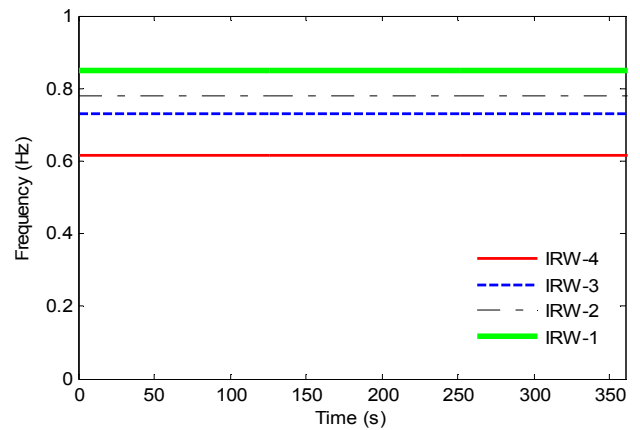
Table 4: Identified modal frequencies

| Region | Wave | Measured (Hz) | |
|-------------|-------|---------------|------------|
| | | TVAR Model | SSI Method |
| WF response | IRW-1 | 0.831 | 0.828 |
| | IRW-2 | 0.785 | 0.781 |
| | IRW-3 | 0.715 | 0.712 |
| | IRW-4 | 0.611 | 0.613 |
| LF response | IRW-1 | 0.052 | 0.051 |
| | IRW-2 | 0.054 | 0.052 |
| | IRW-3 | 0.051 | 0.053 |
| | IRW-4 | 0.053 | 0.054 |

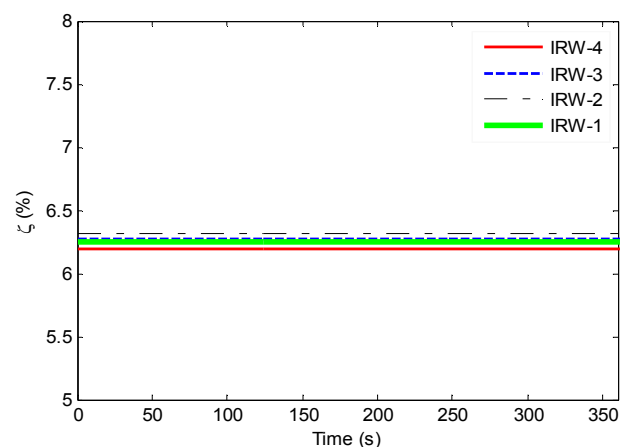
The differences are 10.3%, 16.36, 18.18% and 24.11%, respectively. It might be the second-order nonlinear effect and hydrodynamic load are more pronounced in waves than still water. Further, discrepancies between TVAR model and SSI method are insignificant.

Table 5: Identified modal damping ratios

| Region | Wave | Measured (%) | |
|-------------|-------|--------------|------------|
| | | TVAR Model | SSI Method |
| WF response | IRW-1 | 6.25 | 6.23 |
| | IRW-2 | 6.32 | 6.33 |
| | IRW-3 | 6.27 | 6.29 |
| | IRW-4 | 6.20 | 6.22 |
| LF response | IRW-1 | 14.89 | 14.90 |
| | IRW-2 | 13.81 | 13.78 |
| | IRW-3 | 13.51 | 13.53 |
| | IRW-4 | 12.56 | 12.54 |



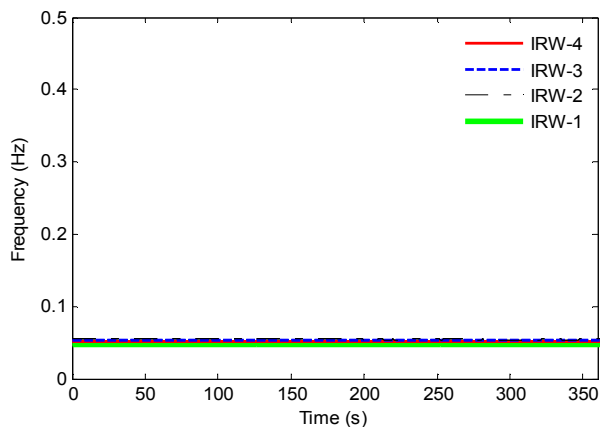
(a)



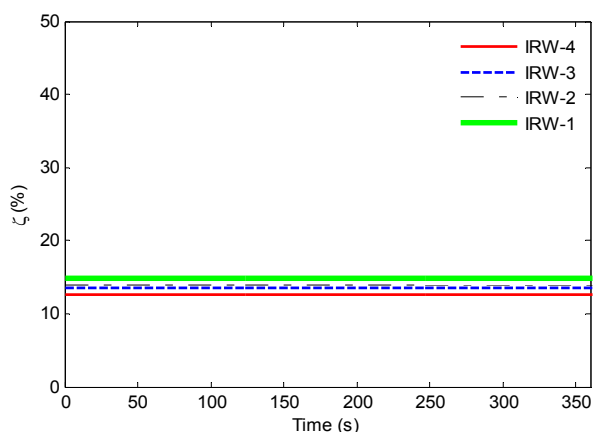
(b)

Fig. 10 Identified time-varying modal analysis in WF region (a) frequency (b) damping ratio

Another advantage of using the TVAR model is that the time evolution of modal properties can be presented. Model order (2,2) for WF and for LF region are chosen for this purpose. The results are presented in Fig. 10 and 11. From the results obtained, it can be observed that semi-submersible model test in the wave tank has a stationary process in WF and LF region. This is to be expected since decomposition process produces stationary time series.



(a)



(b)

Fig. 11 Identified time-varying modal analysis in LF region
(a) frequency (b) damping ratio

V. CONCLUSION

In this paper, a parametric approach for modal properties estimation is presented by using output only measurement. Decomposition of the surge response is carried out to identify WF or LF motion using EMD method. Modal analysis becomes much easier to be carried out to the decomposed surge response. It is found out that the proposed method produces accurate result in estimating response frequencies either in WF or LF region. Damping ratios in LF region and free-decay test are at least twice of values in the WF region. Further, free decay test might underestimate the damping ratio

of the model. The minimum discrepancy is about 10.3% and higher as wave frequency increases. SSI method as a benchmark also confirms the accuracy of the proposed approach. All the results have proven that the proposed EMD-based TVAR model can effectively identify the dynamic characteristics of semi-submersible under wave run-up. The methodology presented in this paper is potential to be used in modal analysis of floating structures. However, the utilization of the results in dynamic response prediction is future work.

ACKNOWLEDGMENT

The authors are thankful to Universiti Teknologi PETRONAS for providing the research facilities.

REFERENCES

- [1] S.L.J. Hu, P. Li, H.T. Vincent, and H.J. Li, "Modal parameter estimation for jacket-type platforms using free-vibration data," *Journal of Waterway, Port, Coastal and Ocean Engineering*, vol. 137(5), pp. 234-245, 2011.
- [2] H.J. Li, P. Li, and S.L.P. Hu, "Modal parameter estimation for jacket-type platforms using noisy free vibration data: sea test study," *Applied Ocean Research*, vol. 37, pp. 45-53, 2012.
- [3] G. Rilling, P. Flandrin and P. Goncalves, "On empirical mode decomposition and its algorithms," in *NSIP-03 2003 IEEE-EURASIP Workshop on nonlinear signal and image processing*.
- [4] R.T. Rato, M.D. Ortigueira, and A.G. Batista, "On the *HHT*, its problems, and some solutions," *Mechanical Systems and Signal Processing*, pp. 1374-1394, vol. 22, 2008.
- [5] E. Yazid, M.S. Liew, P. Setyamartana and V.J. Kurian, "Field measurements based RAO estimation via the TVAR model," in *Proc. 31th International Conference on Offshore, Mechanic and Arctic Engineering*, 2012, pp. 180-187.
- [6] A.G. Poulimenos and S.D. Fassois, "Parametric time-domain methods for non-stationary random vibration modeling and analysis," *Mechanical Systems and Signal Processing*, pp. 763-816, vol. 20, 2006.
- [7] M.A. Yassir, V.J. Kurian and I.S. Harahap, "Second order motion responses of semi-submersibles: numerical and experimental study," in *Proc. 21th International Offshore and Polar Engineering Conference*, 2011, pp. 588-595.
- [8] Y. Birkelund, E.J. Powers and A. Hanssen, "On the estimation of nonlinear Volterra models in offshore engineering," in *Proc. 12th International Offshore and Polar Engineering Conference*, 2002, pp. 180-187.
- [9] P.D. Spanos, R. Ghosh, L.D. Finn, and J.E. Halkyard, "Coupled analysis of a spar structure: Monte Carlo and statistical linearization solutions," *Journal of Offshore Mechanics and Arctic Engineering*, ASME pp. 11-16, vol. 127, 2005.
- [10] Y.M. Low and R.S. Langley, "Understanding the coupling effects in deep water floating structures using a simplified model," *Journal of Offshore Mechanics and Arctic Engineering*, ASME, pp. 1-10, vol. 130, 2008.